



Earliest Holocene deglaciation of the central Uummannaq Fjord system, West Greenland

WILLIAM PHILIPPS , JASON P. BRINER, OLE BENNIKE , AVRIEL SCHWEINSBERG, CASEY BEEL AND NATHANIEL LIFTON

BOREAS



Philipps, W., Briner, J. P., Bennike, O., Schweinsberg, A., Beel, C. & Lifton, N. 2018 (January): Earliest Holocene deglaciation of the central Uummannaq Fjord system, West Greenland. *Boreas*, Vol. 47, pp. 311–325. <https://doi.org/10.1111/bor.12270>. ISSN 0300-9483.

Uummannaq Fjord, West Greenland, held the Uummannaq Ice Stream system that drained an estimated ~6% of the Greenland Ice Sheet (GrIS) during the Last Glacial Maximum. Published ages for the final deglaciation in Uummannaq Fjord vary from as early as *c.* 9.8 ka to as late as *c.* 5.3 ka. Assessing this variability requires additional chronological controls to improve the deglaciation history of central West Greenland. Here, we combine ^{14}C dating of lake sediment cores with cosmogenic ^{10}Be exposure dating at sites adjacent to the present GrIS margin in the central-inland sector of the Uummannaq Fjord system. We find that ice retreated to or within the present GrIS margin at 10.8 ± 0.2 ka ($n = 6$). Although this 'final deglaciation' to or within the present GrIS margin across the Uummannaq Fjord system varies from *c.* 10.8 to 5.3 ka, all chronologies indicate collapse from the continental shelf to the inner fjords at *c.* 11.0 ka, which occurred at a net retreat rate of 300–1100 m a^{-1} . The Uummannaq Fjord system deglaciated *c.* 1000 years earlier than the major fjord system to the south, Disko Bugt. However, similarly rapid retreat rates of the two palaeo-ice stream systems suggest that their collapse may have been aided by high calving rates. The asynchronous deglaciation of the GrIS throughout the Uummannaq Fjord system probably relates to the influence of varying fjord geometry on marine glacier behaviour.

William Philipps (philippswill@gmail.com), Jason P. Briner and Avriel Schweinsberg, Department of Geology, University at Buffalo, Buffalo, NY 14260, USA; Ole Bennike, Geological Survey of Denmark and Greenland, Øster Voldgade 10, Copenhagen K 1350, Denmark; Casey Beel, Department of Geography and Planning, Queen's University, Bruce Wing/Miller Hall, 36 Union Street, Kingston, ON K7L 3N6, Canada; Nathaniel Lifton, Department of Earth, Atmospheric and Planetary Sciences, Purdue University, 550 Stadium Mall Drive, West Lafayette, IN 47907, USA; received 24th August 2016, accepted 2nd June 2017.

Ice-sheet reconstructions extend the history of glacier behaviour beyond the instrumental record and during climatic conditions that are more variable than what exists in the observational period (e.g. Overpeck *et al.* 2006; Alley *et al.* 2010). The Greenland Ice Sheet (GrIS) is relatively sensitive to global climate events and experienced significant fluctuations since the Last Glacial Maximum at 26–19 ka (LGM; Clark *et al.* 2009). Overall, the GrIS experienced variable rates of retreat during deglaciation, was smaller than present during the middle Holocene thermal maximum, and since that time has expanded (e.g. Funder *et al.* 2011; Larsen *et al.* 2015; Young & Briner 2015). Re-advances and stand-stills of the GrIS in response to short-lived climate events punctuated the overall pattern of retreat during the early Holocene and lend insight into the time scale of GrIS response to climate change (e.g. Young *et al.* 2013a). However, there remain many factors that influence the response of the GrIS to climate change on both decadal and millennial time scales, and reconstructing the ice sheet's history can help to unravel its complex behaviour.

Final deglaciation ages when the margin of the GrIS attained a position similar to the present position along the west coast of Greenland show a complex and variable pattern. The oldest ages occur in Southwest (*c.* 10.8–10.1 ka) and Northwest Greenland (*c.* 10.7 and 9.6 ka) (Fig. 1; Bennike & Björck 2002; Briner *et al.* 2013; Carlson *et al.* 2014; Sinclair *et al.* 2016). In central West

Greenland, within the Uummannaq Fjord system alone, where there is a high density of outlet glaciers (Reeh 1985; Velicogna & Wahr 2006), deglaciation ages are highly variable across a relatively small region. The existing chronologies from within the Uummannaq Fjord system focus on post-LGM deglaciation and place the GrIS retreating up to its historical ice limit at Inngia Fjord by *c.* 9.8 ka (Lane *et al.* 2014) and up to Store Gletscher by *c.* 8.7 ka (Roberts *et al.* 2013). However, the deglaciation ages at Rink Isbræ are much younger; there, deglaciation occurred as late as *c.* 5.3 ka (Lane *et al.* 2014).

The variation in final deglaciation ages within the Uummannaq Fjord system is greater than other regions on Greenland (Sinclair *et al.* 2016) and requires additional chronological controls to more fully comprehend. Here, we combine ^{14}C dating of lake sediment cores with cosmogenic ^{10}Be exposure dating (hereafter referred to as ^{10}Be dating) of erratic boulders and bedrock outcrops at two previously uninvestigated sites adjacent to the present GrIS margin in the central-inland sector of the Uummannaq Fjord system. Our primary goal is to add to the chronology for the timing of final deglaciation of the Uummannaq Ice Stream system that occupied the Uummannaq Fjord system during the LGM. A secondary goal is to examine sediment records from ice sheet fed lakes to better understand the Holocene history of the central Uummannaq Fjord region.

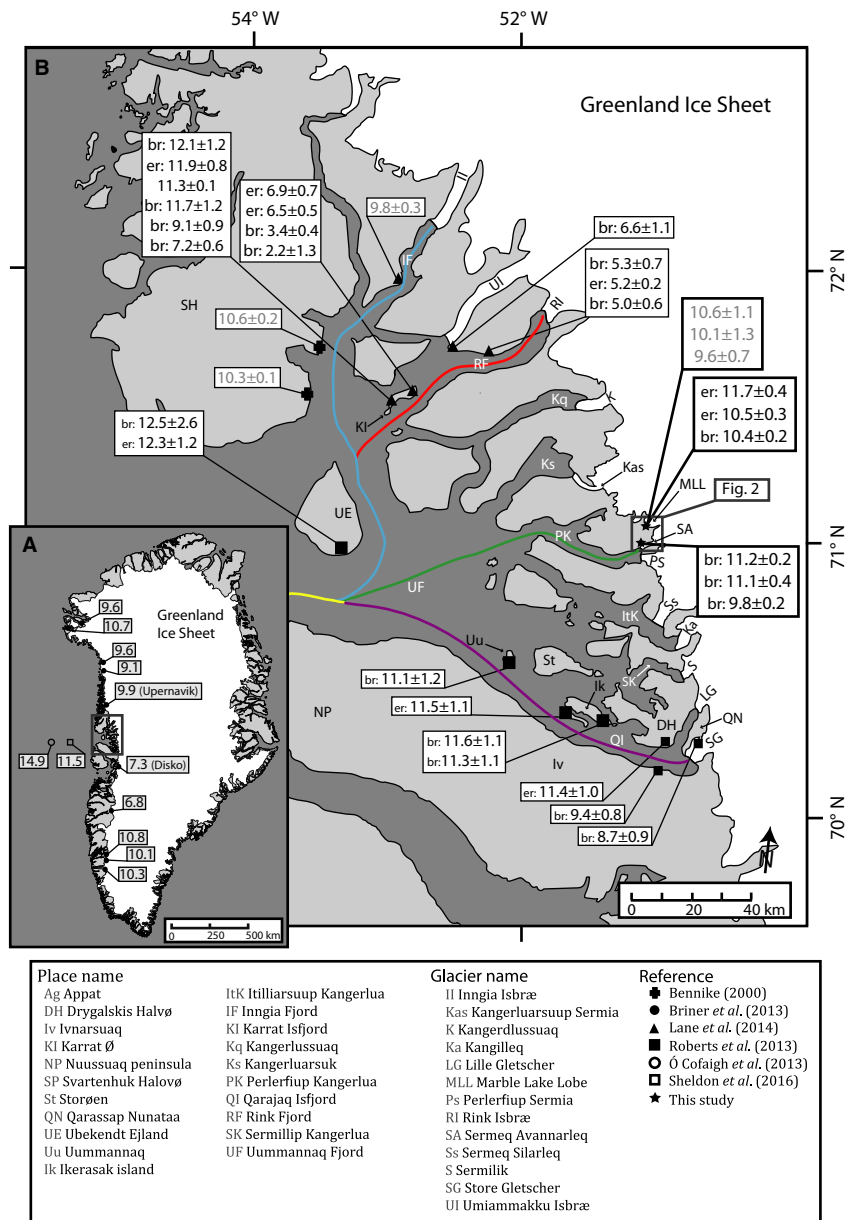


Fig. 1. A. Index map of Greenland showing the GrIS and representative deglaciation ages (in ka) in western Greenland (from Weidick (1978), Fredskild (1985), Bennike (2008), Levy *et al.* (2012), Weidick *et al.* (2012), Young *et al.* (2013a) and Larsen *et al.* (2014)). B. Map of the Uummannaq region showing place names and a summary of ages with no assumed inheritance ages (grey text: ^{14}C ages, black text: cosmogenic nuclide exposure ages) constraining early Holocene retreat of the Uummannaq Ice Stream system. Multi-coloured lines represent the deglaciation through the sub-fjords depicted in Fig. 10. [Colour figure can be viewed at www.boreas.dk]

Material and methods

^{10}Be dating

We dated samples outboard of Sermeq Avannarleq ($n = 3$) and the Marble Lake Lobe (informal name; $n = 3$) ~5 km northeast of Sermeq Avannarleq, using ^{10}Be dating (Figs 2, 3). The upper several centimetres of bedrock and boulder surfaces were collected using a hammer and chisel. All bedrock samples showed signs of glacial polish, and erratic boulders, with smooth sur-

faces, were perched on glacially polished bedrock. A handheld GPS receiver with a vertical uncertainty of ± 4 m was used to record sample location and elevation. A clinometer was used to measure shielding from the surrounding topography. Within a few metres distal to the right lateral moraines that we believe mark the Little Ice Age (LIA) limit of Sermeq Avannarleq, are samples 13GROr-77 and 13GROr-78. Sample 13GRSA-05 is from above the left lateral LIA moraine of Sermeq Avannarleq. The three samples are from glacially polished quartz veins occurring in schistose bedrock.

At the Marble Lake Lobe, we report three ^{10}Be ages collected to the west of a lake informally named Erratic Lake. Sample 13GROr-73 is a boulder perched on polished bedrock and samples 13GROr-75 (erratic) and 13GROr-76 (bedrock) are a paired sample set within several metres of one another, both of gneissic composition. Topographical correction factors were calculated using <http://hess.ess.washington.edu/math> Version 2.2 (Balco *et al.* 2008) and range from 0.9973 to 0.9999 (Table 1).

Physical and chemical processing of all but one sample took place at the University of Buffalo using the methods reported in Young *et al.* (2013b). Sample 13GRSA-05 was processed at PRIME Lab, Purdue University, using procedures outlined in Lifton *et al.* (2014). Beryllium ratios for all but one sample were measured at the Lawrence Livermore National Laboratory's Center for Accelerator Mass Spectrometry, and sample 13GRSA-05 was measured at PRIME Lab. All samples were compared against the 07KNSTD

standard with a reported ratio of 2.85×10^{-12} (Nishiizumi *et al.* 2007; Rood *et al.* 2010) and background was corrected using procedural blanks (Table 1). ^{10}Be ages were calculated using the CRONUS-Earth online exposure age calculator <http://hess.ess.washington.edu/math> Version 2.2 (Balco *et al.* 2008), applying a locally calibrated ^{10}Be production rate from Baffin Bay (Briner *et al.* 2012; Young *et al.* 2013b) with the Lal/Stone (Lm) scaling scheme (Lal 1991; Stone 2000). No corrections for snow cover were made on any of the samples based on the assumption that the area remains windswept due to strong katabatic winds. The presence of polished bedrock surfaces indicates negligible post-glacial erosion.

Lake sediment coring

We cored three lakes within a $\sim 0.75\text{-km}$ radius of one another in a glacially sculpted Precambrian crystalline bedrock landscape that includes a layer of marble

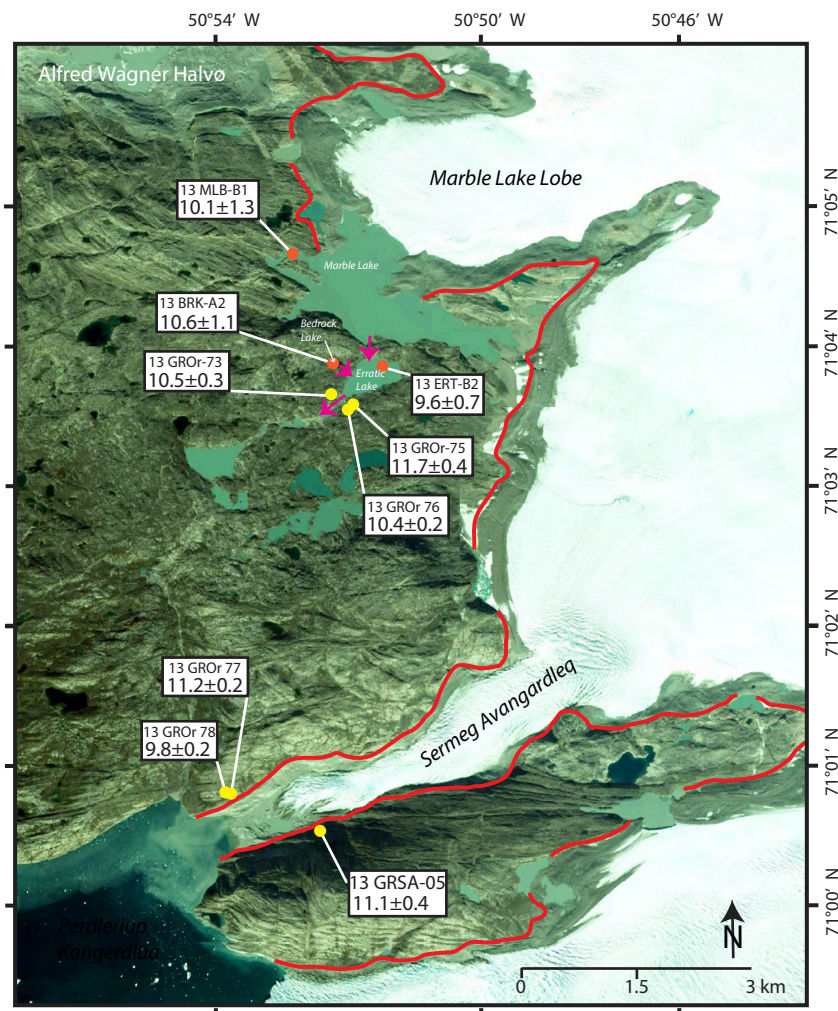


Fig. 2. The study area showing location of ^{10}Be ages in ka (yellow dots) and coring locations and lowest ^{14}C ages in sediment cores (red dots). The LIA moraine/trimline is indicated with the red line. The base image is from Google Earth. [Colour figure can be viewed at www.boreas.dk]

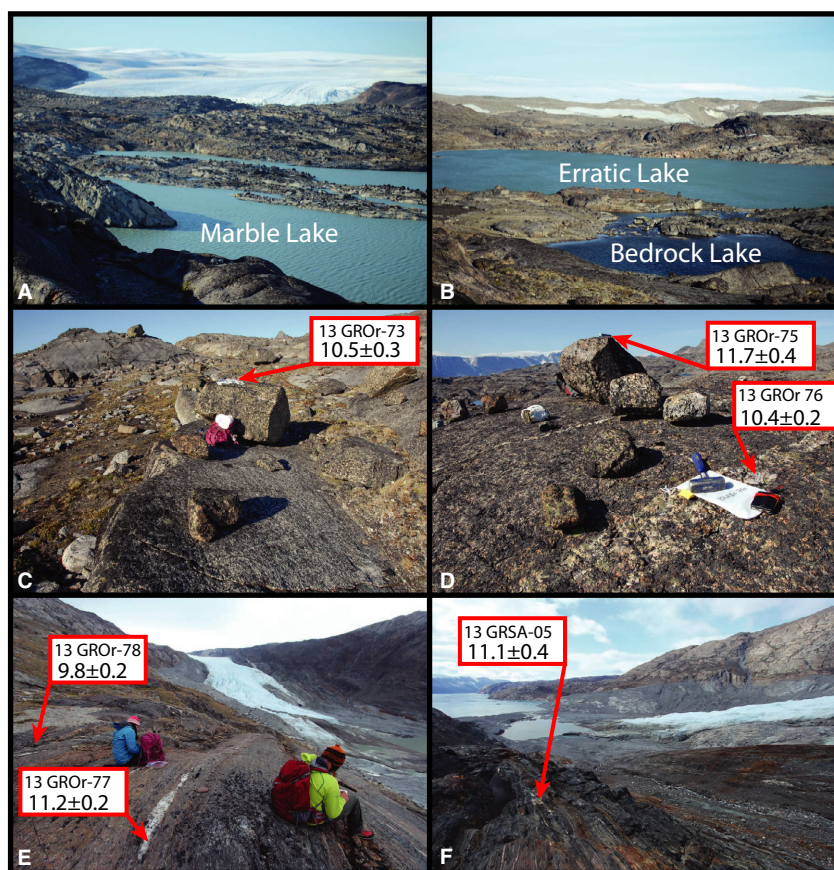


Fig. 3. A. Western portion of Marble Lake (informal name). In the middle ground is the back distal basin of the lake where sediment core 13MBL-B1 was retrieved. B. Image of Erratic and Bedrock lakes (informal names) where sediment cores 13ERT-B2 and 13BRK-A2 were obtained. C. The collection site southwest of Erratic Lake. Samples are from a gneissic erratic boulder (13GRO-75) next to an *in situ* quartz vein (13GRO-76). D. Gneissic erratic bolder (13GRO-73) southeast of Erratic Lake. E. *In situ* quartz veins (13GRO-77 and 13GRO-78) west of Sermeq Avangardleq collected above the left lateral LIA trim zone. F. *In situ* quartz veins west of Sermeq Avangardleq collected above the right lateral LIA trim zone. All ages in ka. [Colour figure can be viewed at www.boreas.dk]

outcropping outboard of the GrIS's present ice margin of the Marble Lake Lobe (Fig. 2). Lake bathymetry to identify local basin centres was determined using an echo-sounder and a weighted tape measure. We collected an 81.7-cm-long sediment core (13MBL-B1) from a

distal sub-basin of Marble Lake (715 m a.s.l.) situated behind a bedrock island separated from the main lake by shallow (~1–2 m) sills. We collected a 109.0-cm-long sediment core (13ERT-B2) from Erratic Lake (701 m a.s.l.). The GrIS presently terminates in Marble Lake,

Table 1. ^{10}Be data for calculation of cosmogenic nuclide exposure ages. Blank-corrected ratios are reported relative to the 07KNSTD standard of 2.85×10^{-12} (Nishiizumi *et al.* 2007; Rood *et al.* 2010). Process blank for this sample batch is 2.877×10^{-15} . We used 0.65 g of 405.2 ppm Be carrier.

Sample	Latitude (°N)	Longitude (°W)	Elevation (m a.s.l.)	Sample type	Thickness (cm)	Shielding correction	Quartz (g)	^9Be carrier (g)	$^{10}\text{Be} \pm 1\sigma$ (10^4 atoms g^{-1})	^{10}Be age (ka)
13GROr-73	71.06837	50.88698	724	Granitic boulder	1	0.9996	35.42	0.6044	9.03E+04	10.5±0.3
13GROr-75	71.06427	50.8853	727	Granitic boulder	2	0.9998	15.10	0.6042	1.00E+05	11.7±0.4
13GROr-76	71.06428	50.88522	727	Bedrock quartz vein	1	0.9998	40.46	0.6071	9.02E+04	10.4±0.2
13GROr-77	71.02202	50.92366	180	Bedrock quartz vein	1	0.9923	80.99	0.6183	5.68E+04	11.2±0.2
13GROr-78	71.02202	50.92373	236	Bedrock quartz vein	1	0.9923	80.11	0.6925	5.26E+04	9.8±0.2
13GRSA-05	71.01771	50.88993	117	Bedrock quartz vein	1	0.9713	85.44	0.7442	4.38E+05	11.1±0.4

which drains into Erratic Lake (Figs 2, 3). We collected a 113.0-cm-long sediment core (13BRK-A2) from a third lake, named Bedrock Lake, which is a non-glacier-fed lake at 702 m a.s.l. adjacent to and draining into Erratic Lake (Figs 2, 3).

Sediment cores were collected using a Universal Coring System, which allowed us to collect the sediment-water interface. Cores that contained excess water above the surface sediments were drained and the sediment-water interface was preserved using the binding agent Zorbitrol (sodium polyacrylate). Cores were packaged tightly and transported to cold storage at the University at Buffalo. Following splitting, photographing and logging to scale, magnetic susceptibility (MS) was measured at 0.5-cm resolution using a Bartington MS2E high-resolution surface-scanning sensor.

We imaged core surfaces using a digital camera and measured MS every 0.2 cm using a Geotek Core Scanner at the University of Massachusetts, Amherst. Also using the Geotek, sediment wet bulk density was measured using a gamma ray logger. Chlorin content, a measure of the primary digestive products of chlorophyll, used as a proxy of a lake's organic productivity (Wolfe *et al.* 2006; Michelutti *et al.* 2010; Boldt *et al.* 2015), was inferred from visible reflectance spectroscopy using the relative absorption bands from 590 to 670 nm following the equation described in Rein & Sirocko (2002). We also measured elemental composition of 13MBL-B1 and 13ERT-B2 using an ITRAX X-ray Fluorescence (XRF) Core-scanner, also at the University of Massachusetts, Amherst. Generator settings for the ITRAX were 60 kV voltage, 50 mA current and 5000 ms exposure time; the data are presented as peak areas of counts per second (cps). We measured the concentrations of 27 different elements. Here we focus on fluctuations of Ti, K, Fe, Si and Ca, used previously to monitor variations of glacial input (Larsen *et al.* 2011; Håkansson *et al.* 2014). Finally, we used loss-on-ignition at 550 °C (LOI₅₅₀) as a measure of organic matter content and loss-on-ignition at 1000 °C (LOI₁₀₀₀) as a measure of CaCO₃ content at contiguous 0.5-cm increments at the University at Buffalo. By combining these data, we characterize the transition of sediment units from and to minerogenic to organic-rich with the goal of tracking ice-margin proximity through the Holocene (e.g. Briner *et al.* 2010).

We obtained 16 ¹⁴C ages in total from the three lakes, from both aquatic macrofossils (n = 15) and a bulk sediment sample (n = 1). Samples were dated at the National Ocean Sciences Accelerator Mass Spectrometry Facility at Woods Hole Oceanographic Institute. The ¹⁴C ages were calibrated using CALIB html version 7.1 using the CALIB13 data set. We report the mean ¹⁴C age by taking the midpoint of the full two standard deviation age range (Table 2).

Age-depth models for cores 13ERT-B2 and 13BRK-A2 were made using the smooth spline and cubic spline functions in R software's CLAM version 3.0.1 code

(<http://chrono.qub.ac.uk/blaauw/clam.html> version 2.2; Blaauw 2010) (Fig. 4). We only obtained two ¹⁴C ages in core 13MBL-B1 from near the contact of major sedimentological shifts, and thus did not generate an age-depth model for this core. The sediment-water interface is preserved in all three cores; therefore we assume a surface age of -63 cal. ka BP in each core.

Results and interpretations

¹⁰Be ages

Six ¹⁰Be ages from Sermeq Avannarleq and adjacent to Erratic Lake sites yielded similar ages (Figs 2, 3). At Sermeq Avannarleq, the bedrock samples from just beyond the historical right lateral moraine yield ages of 11.2±0.2 ka (13GROr-77) and 9.8±0.2 ka (13GROr-78). Above the left lateral moraine, the bedrock sample yields an age of 11.1±0.4 ka (13GRSA-05) (Table 1). Near Erratic Lake, two erratic boulders yield ages of 10.5±0.3 ka (13GROr-73) and 11.7±0.4 ka (13GROr-75); one bedrock sample is 10.4±0.2 ka (13GROr-76) (Table 1). The three ¹⁰Be ages from Sermeq Avannarleq average 10.7±0.3 ka; the three ¹⁰Be ages adjacent to Erratic Lake average to 10.9±0.3 ka. The average of all six ¹⁰Be ages is 10.8±0.2 ka. We suggest that the timing of deglaciation at these two sites in the central Uummannaq Fjord system was simultaneous (within the resolution of the ¹⁰Be age uncertainty) at c. 10.8 ka.

Lake sediment records

Bedrock Lake (core 13BRK-A2). – This 113-cm-long sediment core contains a basal unit of mineral-rich sediment overlain by an organic-rich sediment unit. At the base, unit B2 is a 7.5-cm-thick, massive mineral-rich unit that is characterized by low LOI₅₅₀, wet bulk density and chlorin values, and high MS values (Figs 5, 6). The transition to the overlying organic-rich sediment unit (B1) is constrained to prior to 10.8±0.3 cal. ka BP from a ¹⁴C age on bulk sediments. We interpret the basal unit B2 to represent the time when the margin of the Marble Lake Lobe was retreating out of Bedrock Lake's small catchment. A sharp contact separates the mineral-rich sediment unit B2 from the overlying organic-rich unit B1 (Figs 5, 6). The lower portion of unit B1 is a 53.5-cm-thick weakly laminated gyttja that shows a sharp increase in LOI₅₅₀, gamma and chlorin, and a drop in MS values (named unit B1b). Above 52 cm depth, the unit (named Unit B1a) comprises macrofossil-rich gyttja that has the highest LOI₅₅₀ as well as relatively high gamma and chlorin values of the core. Unit B1 represents a time of ice-free conditions between deglaciation and the present day.

Marble Lake (core 13MBL-B1). – This 81.7-cm-long core can be divided into three units. From the bottom,

Table 2. ^{14}C ages from lake sediment cores.

Core name	Depth (cm)	Lab. ID number	Material dated	$\delta^{13}\text{C}$ (‰)	Fraction modern	Radiocarbon age (^{14}C a BP)	Calibrated age (cal. a BP)	Calibrated 2σ age range (cal. a BP)
Bedrock Lake (702 m a.s.l., 71.07012°N, 50.88745°W)								
13 BRK-A2	12.0–12.5	OS-116943	Aquatic macrofossils	-28.89	0.8889±0.0018	945±15	849±40	796–875
13 BRK-A2	36.5–37.0	OS-116944	Aquatic macrofossils	-29.99	0.7070±0.0016	2780±20	2873±75	2798–2948
13 BRK-A2	62.0–62.5	OS-116879	Aquatic macrofossils	-30.85	0.4240±0.0015	6890±30	7729±61	7668–7790
13 BRK-A2	71.5–72.0	OS-116945	Aquatic macrofossils	-15.45	0.3841±0.0016	7690±35	8478±67	8411–8545
13 BRK-A2	78.5–79.0	OS-117188	Chironomids and algae	-17.59	0.3441±0.0031	8570±75	9583±149	9434–9731
13 BRK-A2	88.0–88.5	OS-117192	Chironomids and algae	-21.24	0.3569±0.003	8270±65	9235±202	9033–9437
13 BRK-A2	101.5–102.5	OS-117183	Aquatic macrofossils	-30.85	0.3224±0.0027	9090±70	10 324±170	10 154–10 493
13 BRK-A2	103.5–105.0	OS-107407	Aquatic macrofossils	-32.12	0.3093±0.003	9420±75	10 750±320	10 430–11 070
Marble Lake (714 m a.s.l., 71.08155°N, 50.90318°W)								
13 MBL-B1	7.5–8.0	OS-107408	Aquatic macrofossils	-30.59	0.7267±0.0039	2560±45	2626±136	2490–2761
13 MBL-B1	63.0–65.0	OS-107529	Aquatic macrofossils	-23.93	0.3287±0.0025	8940±60	10 030±204	9826–10 234
Erratic Lake (701 m a.s.l., 71.06972°N, 50.86690°W)								
13 ERT-B2	13.5–14.0	OS-107409	Aquatic macrofossils	-25.33	0.8351±0.0039	1450±37	1348±52	1296–1400
13 ERT-B2	28.0–28.5	OS-107811	Aquatic macrofossils	-24.84	0.5209±0.0018	5240±25	6049±126	5923–6175
13 ERT-B2	40.5–41.0	OS-107411	Aquatic macrofossils	-26.98	0.4480±0.0024	6450±45	7355±77	7278–7432
13 ERT-B2	49.0–49.5	OS-116880	Aquatic macrofossils	-29.41	0.3599±0.0015	8210±35	9157±125	9032–9282
13 ERT-B2	54.0–54.5	OS-107412	Aquatic macrofossils	-31.02	0.3642±0.0027	8110±60	9064±203	8861–9267
13 ERT-B2	60.0–61.0	OS-107530	Bulk sediment	-27.28	0.3421±0.0028	8620±65	9623±139	9484–9762

unit M3 is a 26.5-cm-thick mineral-rich sediment unit with low LOI_{550} , gamma and chlorin values (Fig. 7). LOI_{1000} and Ca steadily increase at the bottom of this unit while Fe, Ti, Si and K remain relatively constant. We interpret the unit as glacier meltwater derived. The increases in Ca and LOI_{1000} most likely result from

ice eroding the local marble outcrops along northern Marble Lake. Above unit M3 is unit M2, which is a 47.0-cm-thick macrofossil-rich layered silty gyttja bracketed by ^{14}C dates of 10.1 ± 0.1 and 2.7 ± 0.1 cal. ka BP on macrofossils near the lower and upper contacts, respectively (Fig. 7). Unit M2 is characterized by relatively

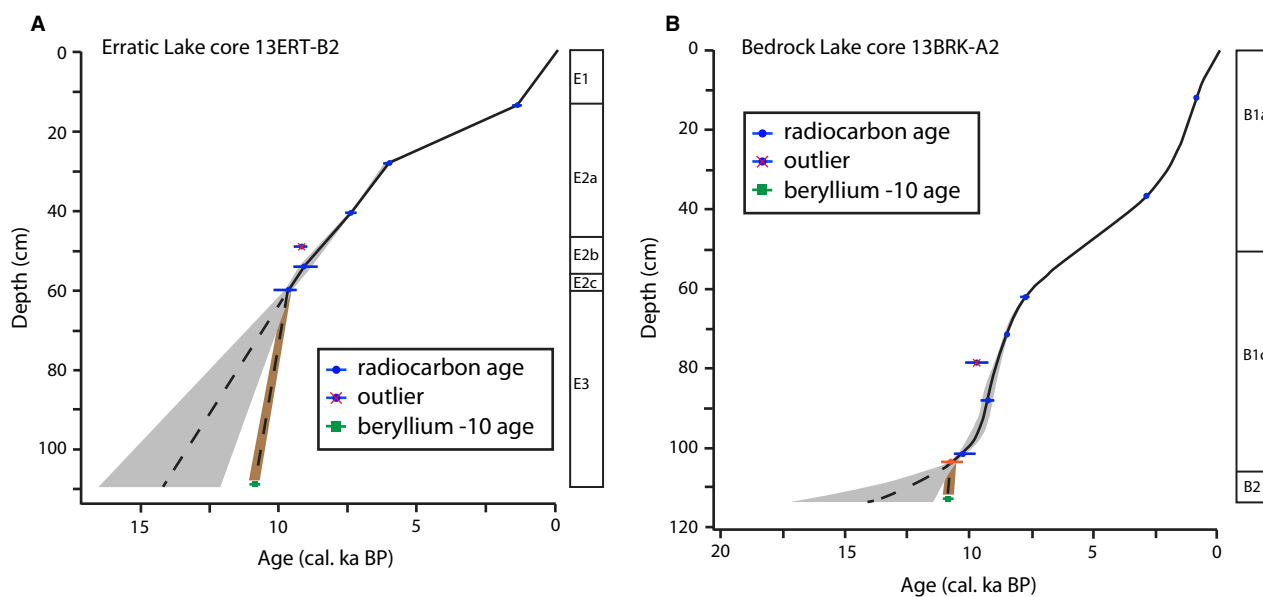


Fig. 4. A. Erratic Lake core 13ERT-B2 age-depth model. B. Bedrock Lake core 13BRK-A2 age-depth model. Lithostratigraphical units are presented on the right side of each panel. Locations of ^{14}C samples are denoted with blue dots for macrofossil age; orange dot is a bulk sediment age. Excluded ages are represented with red 'x'; the ^{14}C ages of 9160 ± 130 cal. ka BP at a depth of 49.0–49.5 cm in core 13ERT-B2 and 9580 ± 150 cal. ka BP at a depth of 78.5–79.0 cm in core 13BRK-A2 are excluded from the age-depth models, due to age reversals. Green rectangles represent the average of all six ^{10}Be ages of 10.8 ± 0.2 ka. Grey polygons represent the modelled ages with no assumptions of basal age and the brown polygons modelled ages with average ^{10}Be ages of 10.8 ± 0.2 ka as a bottom of core age constraint. [Colour figure can be viewed at www.boreas.dk]

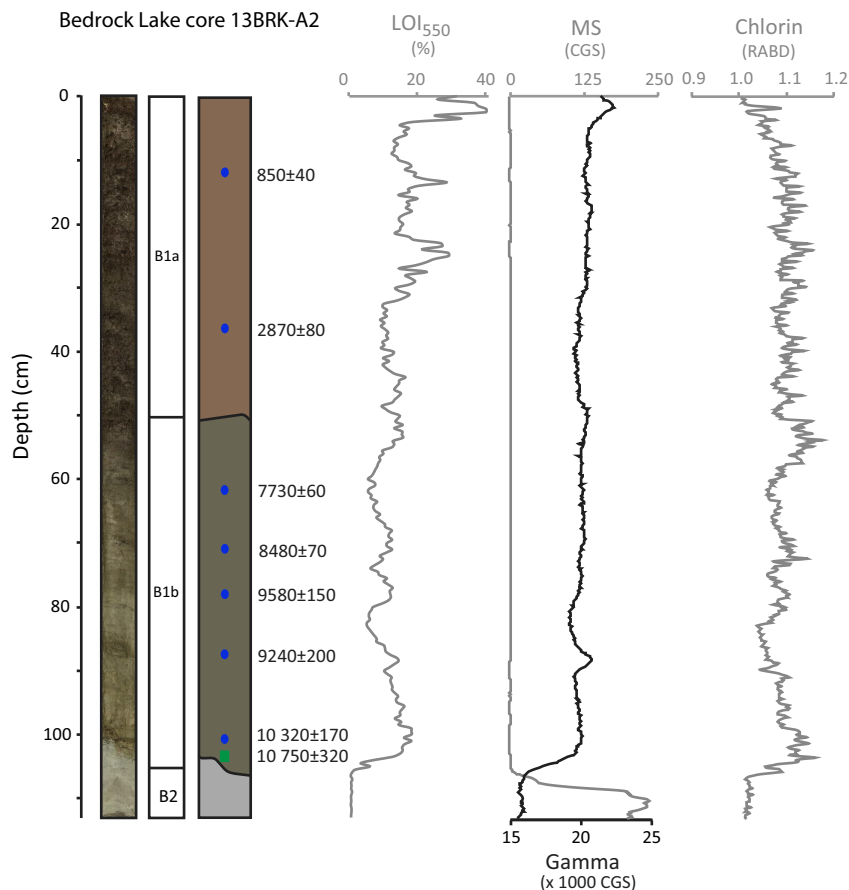


Fig. 5. Bedrock Lake core 13BRK-A2: spliced photograph and lithostratigraphical units are presented on the left side of each panel. The locations of ^{14}C samples and calibrated ages are indicated with blue circles. Physical and geochemical data from the core are plotted as a function of depth; lines are black and grey simply for clarity. [Colour figure can be viewed at www.boreas.dk]

high LOI_{550} , gamma and chlorin values and a corresponding decrease in LOI_{1000} , MS, Si, Ti, K and Ca values. We suggest that unit M2 represents a time when ice receded out of the catchment to an unknown distance behind the present ice margin at or slightly before 10.0 ± 0.1 cal. ka BP.

The uppermost unit, unit M1, is 8.0 cm thick and composed of silt and clay without macrofossils and with laminations occurring at the base of the unit. We interpret unit M1 to span the last *c.* 2650 years. LOI_{550} , gamma and chlorin values are low, while MS, Fe, Si, Ti and K values are relatively high in this unit. We interpret this unit to represent a time when the Marble Lake Lobe resided in Marble Lake's catchment or in the lake.

Erratic Lake (core 13ERT-B2). – The 109.0-cm-long sediment core from Erratic Lake contains three main units. From the bottom, unit E3 is a 49.0-cm-thick mineral-rich unit characterized by relatively high LOI_{1000} , gamma, Si, K and Ca values as well as extremely low LOI_{550} , chlorin and Fe values (Figs 8, 9). A ^{14}C age from the overlying unit E2c constrains the age of the upper contact of unit E3 to before 9.6 ± 0.1 cal. ka BP. We

interpret unit E3 to represent a time of glacial meltwater input that is related to the basal units in Bedrock and Marble Lakes.

Unit E2 lies above unit E3, and is an organic-rich 46.5-cm-thick unit that we divide into three subunits that together span from 9.6 ± 0.1 to 1.4 ± 0.1 cal. ka BP. Unit E2c is a 2.5-cm-thick unit that spans from *c.* 9.6 to 9.5 cal. ka BP and consists of an organic-rich gyttja with high LOI_{550} and chlorin values, and relatively low LOI_{1000} , MS, Fe, Ti, Si, Ca and K values. This unit is interpreted as representing a time when the Marble Lake Lobe retreated out of the catchment of Marble and Erratic lakes. The time of that transition may be better constrained in the Marble Lake core, due to proximity of the ^{14}C age to sediment shift, where it is dated to before 10.1 ± 0.1 cal. ka BP. Unit E2b spans from 10.0 cm (*c.* 9.5–8.4 cal. ka BP) and is silty gyttja with aquatic macrofossils but relatively low LOI_{550} and chlorin values, and relatively high MS, Fe, Ti, Si, K and Ca values. Unit E2b is interpreted to represent a time of lower biological activity, due to significant drops in LOI_{550} and chlorin values relative to Units E2c and E2a. Unit E2a spans from 34.0 cm (*c.* 8.3–1.3 cal. ka

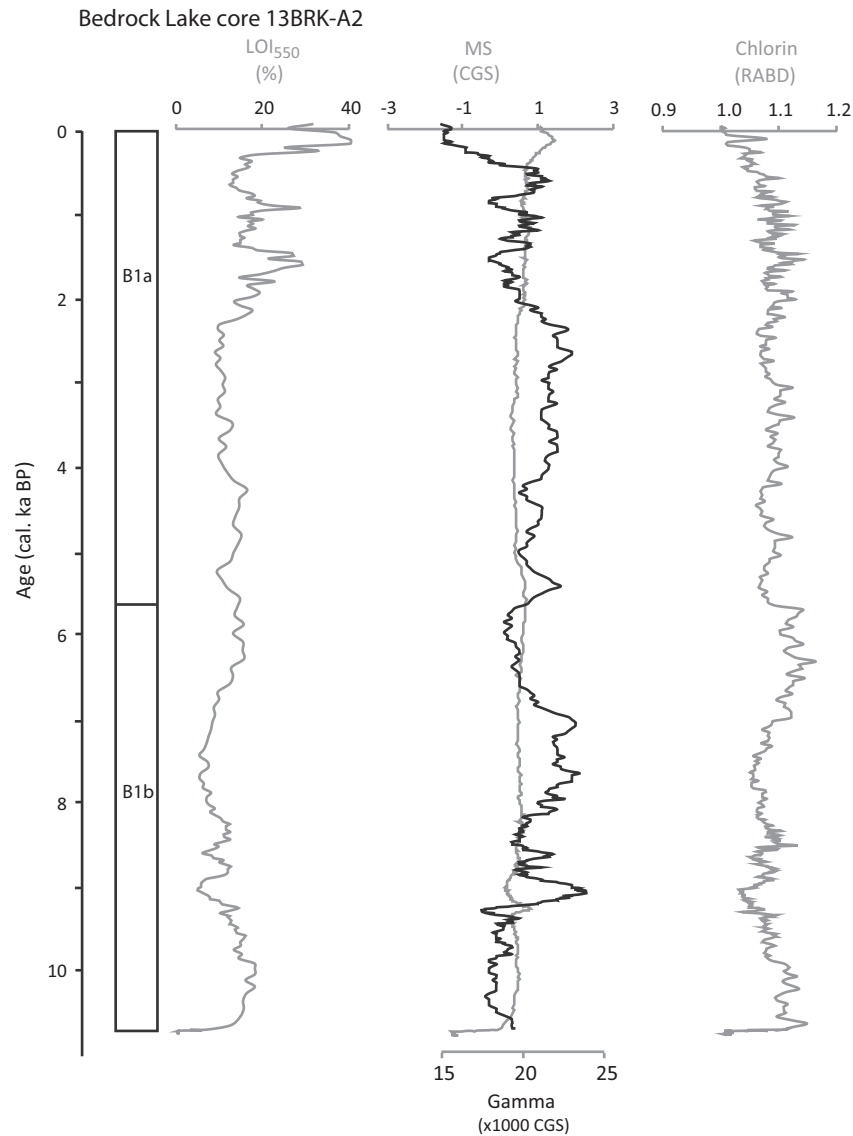


Fig. 6. Sedimentological data for core 13BRK-A2 core plotted vs. age from Bedrock Lake. Lithostratigraphical units are presented on the left side of each panel using in the age depth model from Fig. 4.

BP) and is characterized by an increase in LOI_{550} and chlorin values and a decrease in Fe, Si, Ti and Ca. Unit E2a represents a time of comparatively high levels of organic productivity due to limited to non-existent input of ice-sheet meltwater.

Overlying the organic-rich unit E2 is unit E1, a massively bedded mineral-rich 13.5-cm-thick unit that spans from before 1.4 ± 0.1 cal. ka BP to present. In Unit E1, LOI_{550} , LOI_{1000} , chlorin and Ca values are relatively low while MS, Fe Si, Ti, and K values are relatively high. Unit E1 represents the advance of the ice-sheet margin back into Erratic Lake's catchment. We interpret this unit to correspond to the same glacial meltwater signal in the top of the Marble Lake core (unit M1), and suggest the younger of the two bracketing ages (in this case the

1.40 ± 0.1 cal. ka BP age from Erratic Lake) is the closer maximum-limiting age for the timing of the ice advance.

Glacier history of the study area

We estimate that deglaciation in our study area occurred *c.* 10.8 ± 0.2 ka based on the ^{10}Be ages. The lowermost ^{14}C age constraint from Bedrock Lake, the only lake with a small catchment and therefore most closely dating the deglaciation of the landscape from where the ^{10}Be ages were obtained, is 10.8 ± 0.3 cal. ka BP. The lowermost ^{14}C age constraints from Marble Lake and Erratic Lake are 10.1 ± 0.1 and 9.6 ± 0.1 cal. ka BP, respectively (Figs 4–9; Table 2). Marble and Erratic Lakes probably record the transition from glacial to non-glacial

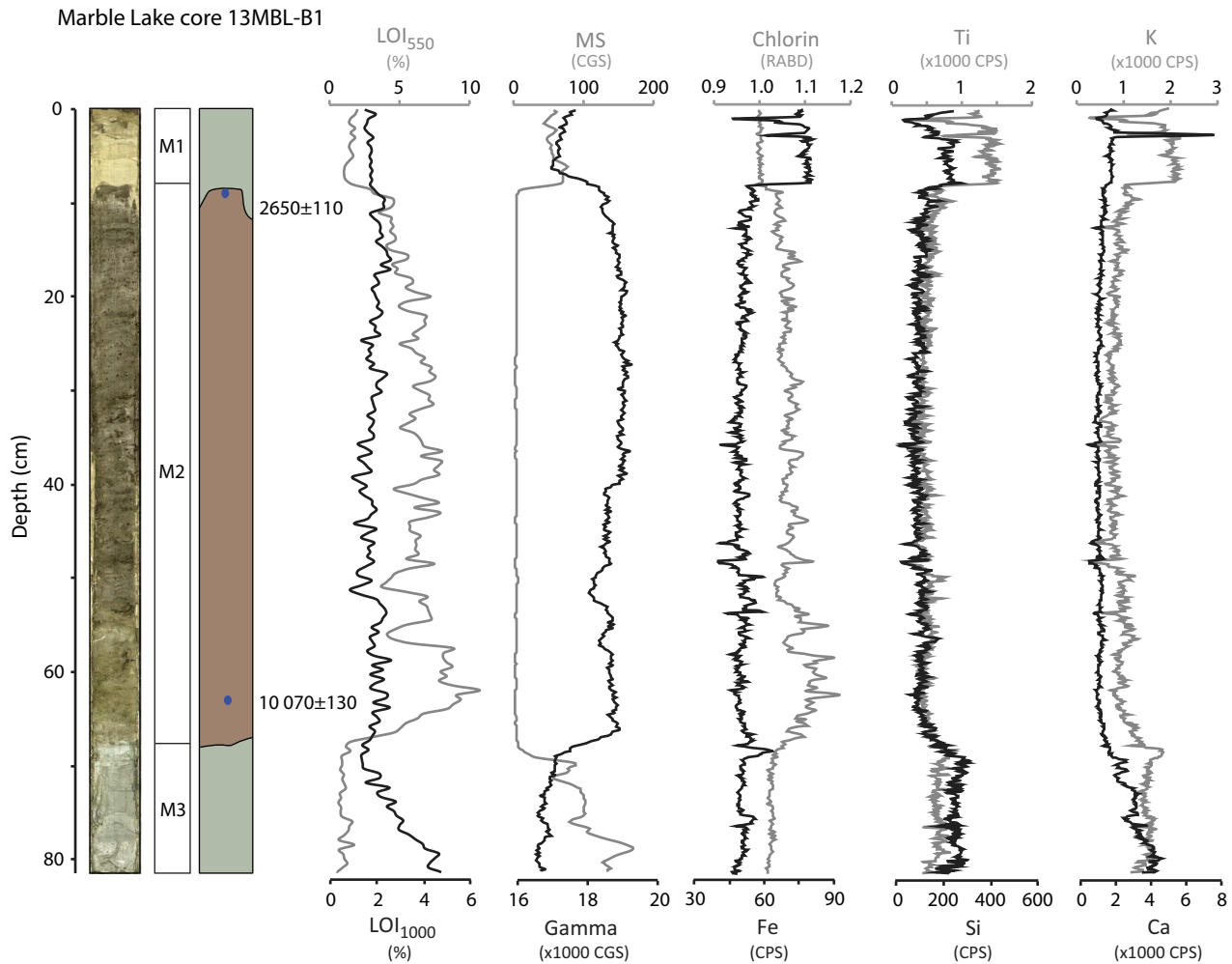


Fig. 7. Marble Lake core 13MBL-B1: spliced photograph and lithostratigraphical units are presented on the left side of each panel. The locations of ^{14}C samples and calibrated ages are indicated with blue circles. Physical and geochemical data from the core are plotted as a function of depth. [Colour figure can be viewed at www.boreas.dk]

sediments later due to their catchments extending eastward beneath the present-day ice-sheet footprint (Morlighem *et al.* 2014).

All three lakes outboard of the Marble Lake Lobe record ice-free to reduced-ice conditions after *c.* 10.8 to *c.* 9.6 cal. ka BP. The Marble Lake sediment record contains an organic-rich unit from *c.* 10.1 to *c.* 2.7 cal. ka BP (unit M2). A decrease in organic matter content in Erratic Lake from *c.* 9.4 to 8.4 cal. ka BP might suggest climatic instability during that time. All three lakes indicate the absence of glacial input until the latest Holocene. Around 2.7–1.4 cal. ka BP (the younger maximum age is probably closer to the sediment transition), the ice margin advanced into the Marble and Erratic Lakes catchments. These lakes are still presently proglacial lakes. Based on LIA trimline zones, we believe the ice-margin advance reached ~ 0.3 km outboard of its present margin and >0.7 km beyond the present terminus of Sermeq Avannarleq (Fig. 2).

Discussion

History of glacier change during the Holocene of the Uummannaq Ice Stream system

Our age of deglaciation of *c.* 10.8 ka for the central Uummannaq Fjord system is similar to the deglaciation at Inngia Isbræ of *c.* 10.6–9.8 cal. ka BP (Figs 1, 10; Bennike 2000; Lane *et al.* 2014). Despite this similarity in deglaciation ages between the two sites, there are differences with the final deglaciation age of Store Gletscher at *c.* 9.4–8.7 ka and Rink Isbræ at *c.* 5.3 ka (Roberts *et al.* 2013; Lane *et al.* 2014). The middle Holocene age for the final deglaciation in this part of Greenland is particularly unusual (e.g. Bennike & Björck 2002). Here, we explore the chronologies from around the Uummannaq Fjord system in more detail in order to understand the apparent asynchronous final deglaciation of the Uummannaq Ice Stream system.

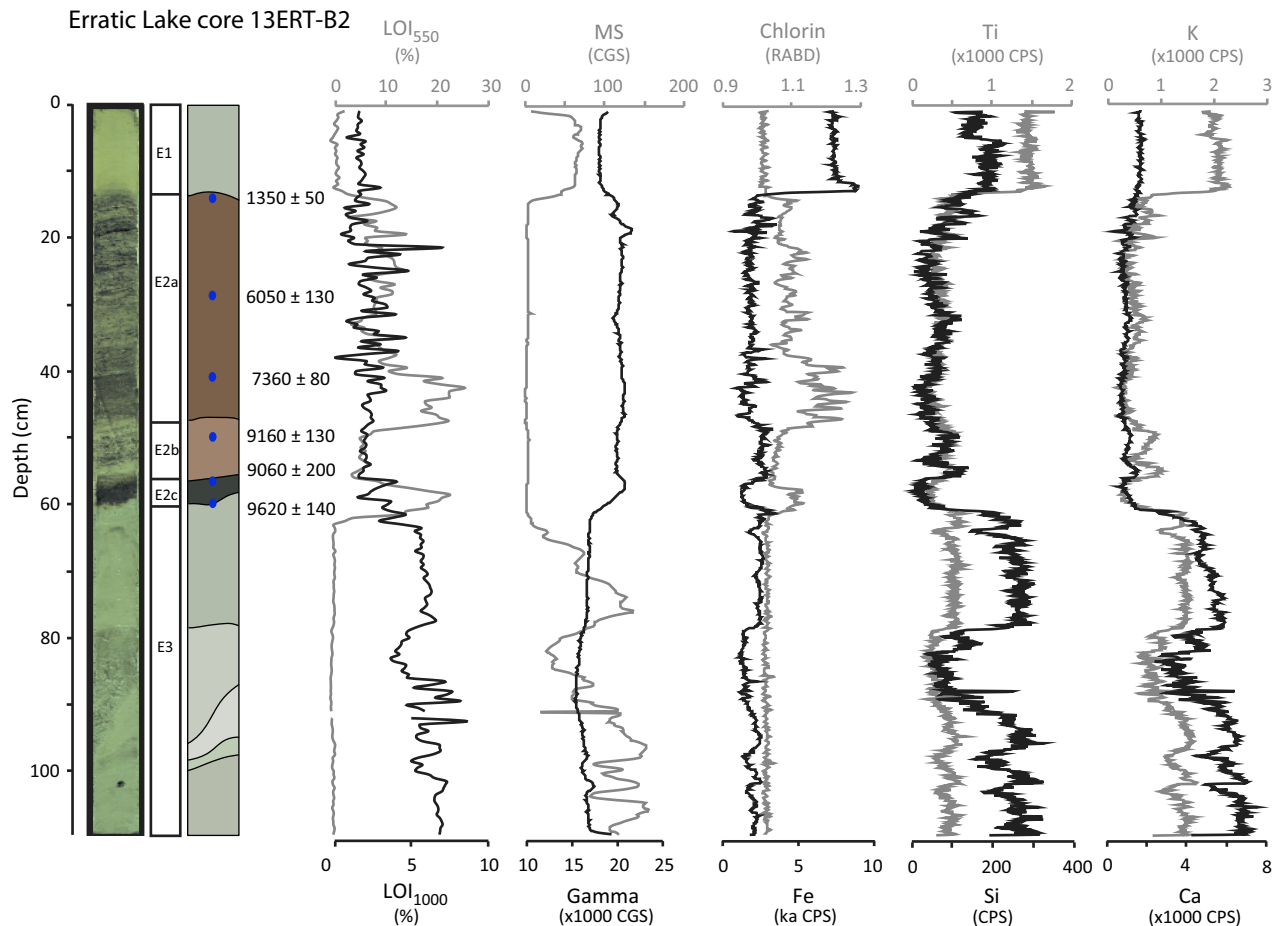


Fig. 8. Erratic Lake core 13ERT-B2: spliced photograph and lithostratigraphical units are presented on the left side of each panel. The locations of ^{14}C samples and calibrated ages are indicated with blue circles. Physical and geochemical data from the core are plotted as a function of depth. [Colour figure can be viewed at www.boreas.dk]

The latest interpretation of ^{14}C ages and sediment packages on the shelf off the Uummannaq Ice Stream system supports the final deglaciation of the shelf following the Younger Dryas, at *c.* 11.5 cal. ka BP (Sheldon *et al.* 2016). In the southern Uummannaq Fjord system, deglaciation through Qarajaq Isfjord occurred around 11.6 ± 1.1 to 11.3 ± 1.1 ka. Near the present ice margin of Lille Gletscher on Drygalskis Halvø, deglaciation occurred by 11.4 ± 1.0 ka (Roberts *et al.* 2013). This suggests rapid deglaciation of >200 km from the mid-shelf to the inner, deep fjords of southern Uummannaq, which is supported by our deglaciation age from the central sector of the Uummannaq Ice Stream system of *c.* 10.8 ka (Figs 1, 10). This episode of rapid deglaciation may have been aided by high calving rates in the deep fjords (800–1200 m b.s.l.) leading to Store Gletscher (Rignot *et al.* 2015, 2016). Following the episode of rapid retreat, there appears to have been a period of stability near the present ice-sheet margin at Store Gletscher, because final deglaciation there occurred after 9.4–8.7 ka (Fig. 1). Although it is only one ^{10}Be age per site, if they accurately record deglaciation,

they suggest a period of ice-margin stabilization that delayed the final deglaciation of Store Gletscher for *c.* 2000 years after the major pulse of retreat (Roberts *et al.* 2013).

Around the time of relative ice-margin stability at Store Gletscher from *c.* 9.4 to *c.* 8.7 ka, the Erratic Lake sediments record climate deterioration (*c.* 9.4–8.4 cal. ka BP). Thus, the Erratic Lake record may support the *c.* 9.4 to 8.7 ka age of ice-margin stabilization near Store Gletscher. Furthermore, this general timing of ice-sheet stability may relate to ice-margin stability elsewhere in western Greenland (e.g. the Mairait moraine, Young *et al.* 2013a; the Drygalski moraines, Cronauer *et al.* 2016).

In northern Uummannaq, there is also evidence for rapid ice retreat from the shelf and into the fjords *c.* 11 ka. Outboard of Inngia Fjord on Svartenhuk Halvø, the existing ages constrain deglaciation to just prior to *c.* 10.3 cal. ka BP (Bennike 2000). Furthermore, the ice retreat to Karrat Ø occurred by *c.* 12–11 ka. This age of deglaciation lies within error of the deglaciation ages from central and southern Uummannaq and

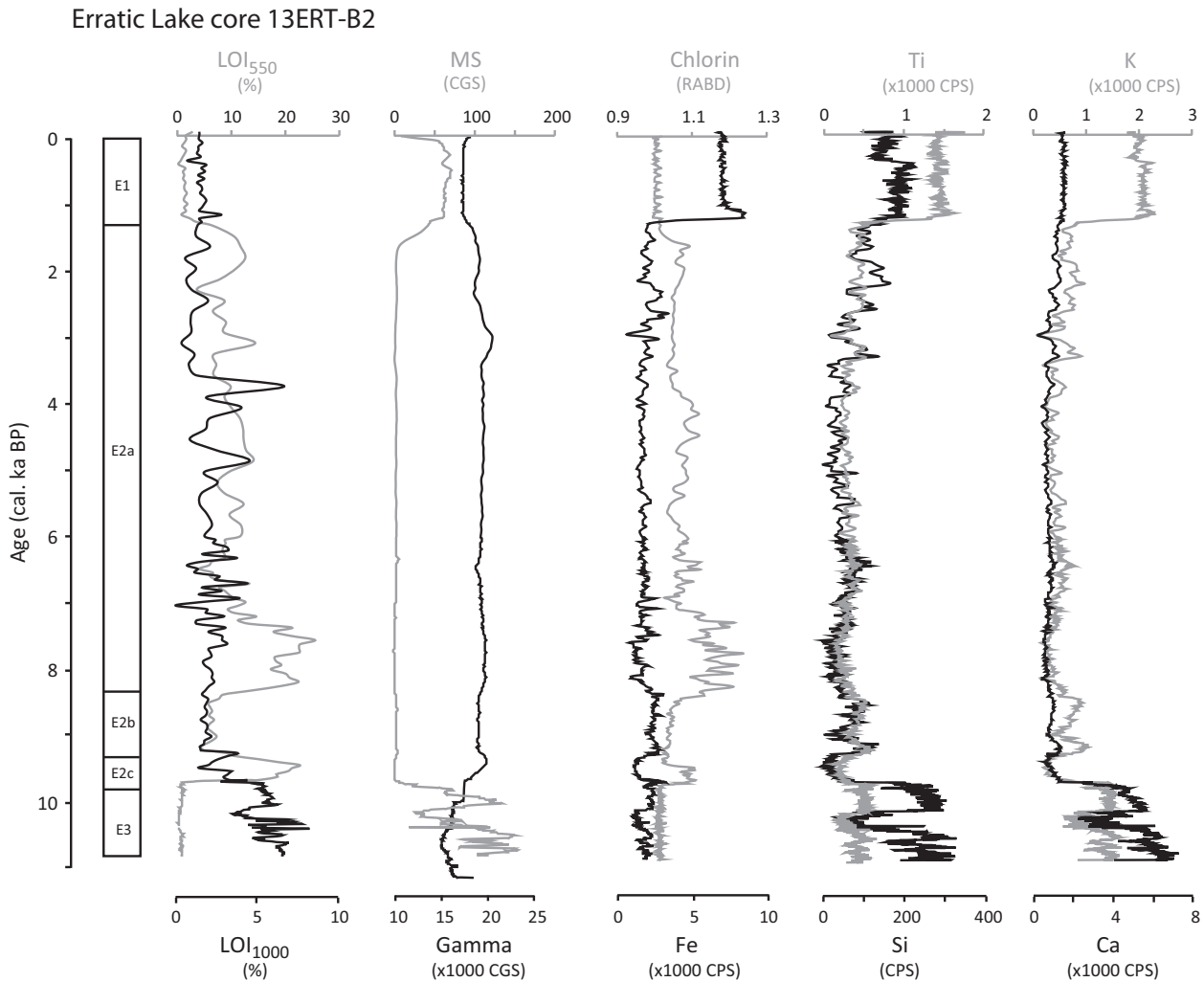


Fig. 9. Erratic Lake core 13ERT-B2: spliced photograph and lithostratigraphical units are presented on the left side of each panel. The locations of ^{14}C samples and calibrated ages are indicated with blue circles. Physical and geochemical data from the core are plotted as a function of age.

supports the rapid retreat of the Uummanaq Ice Stream system following the Younger Dryas from the shelf to the inner fjords (Figs 1, 10; Sheldon *et al.* 2016).

Although there is strong agreement in the timing of deglaciation of southwestern Karrat Ø with elsewhere around the Uummanaq Fjord system, the timing of subsequent deglaciation through Kangilleq fjord is different. The Karrat-Nuugaatsiaq moraines preserved on the low-elevation eastern end of the island demarcate a palaeo-ice margin across central Karrat Ø that dates to *c.* 7–6 ka (Lane *et al.* 2014). The ages of 5.2 ± 0.2 ka ($n = 3$) in mid-Kangilleq fjord constrain the ice retreat toward the present position of Rink Isbræ, ~50 km east of Karrat Ø. The chronology suggests that the GrIS either persisted on, or re-advanced to, eastern Karrat Ø during the middle Holocene, and retreated to or within its present position between after 5 ka.

The pattern of ice residing on Karrat Ø, ~50 km beyond its present position, during the middle Holocene

is anomalous when compared to the deglaciation pattern within the Uummanaq Fjord system and elsewhere on Greenland (e.g. Bennike 2000; Funder *et al.* 2011; Briner *et al.* 2013; Roberts *et al.* 2013). The reason for this anomalous pattern is unknown, but it may relate to topographical/bathymetric controls and the fjord geometry (Lane *et al.* 2014). For example, fjords are narrower to the north and south of Karrat Ø than they are farther west and east (Figs 1, 10). In addition, the fjord inland from Karrat Ø not only widens, but it transitions from ~400 to 500 m deep to >1000 m deep (Rignot *et al.* 2016). Thus, once ice retreated from Karrat Ø, it probably would have receded quickly via rapid calving through this major over-deepening until reaching shallower waters, which exist near and behind the present position of Rink Isbræ (Morlighem *et al.* 2014; Rignot *et al.* 2015, 2016). The cause for this unusual period of middle Holocene stability followed by >50 km of ice-sheet recession

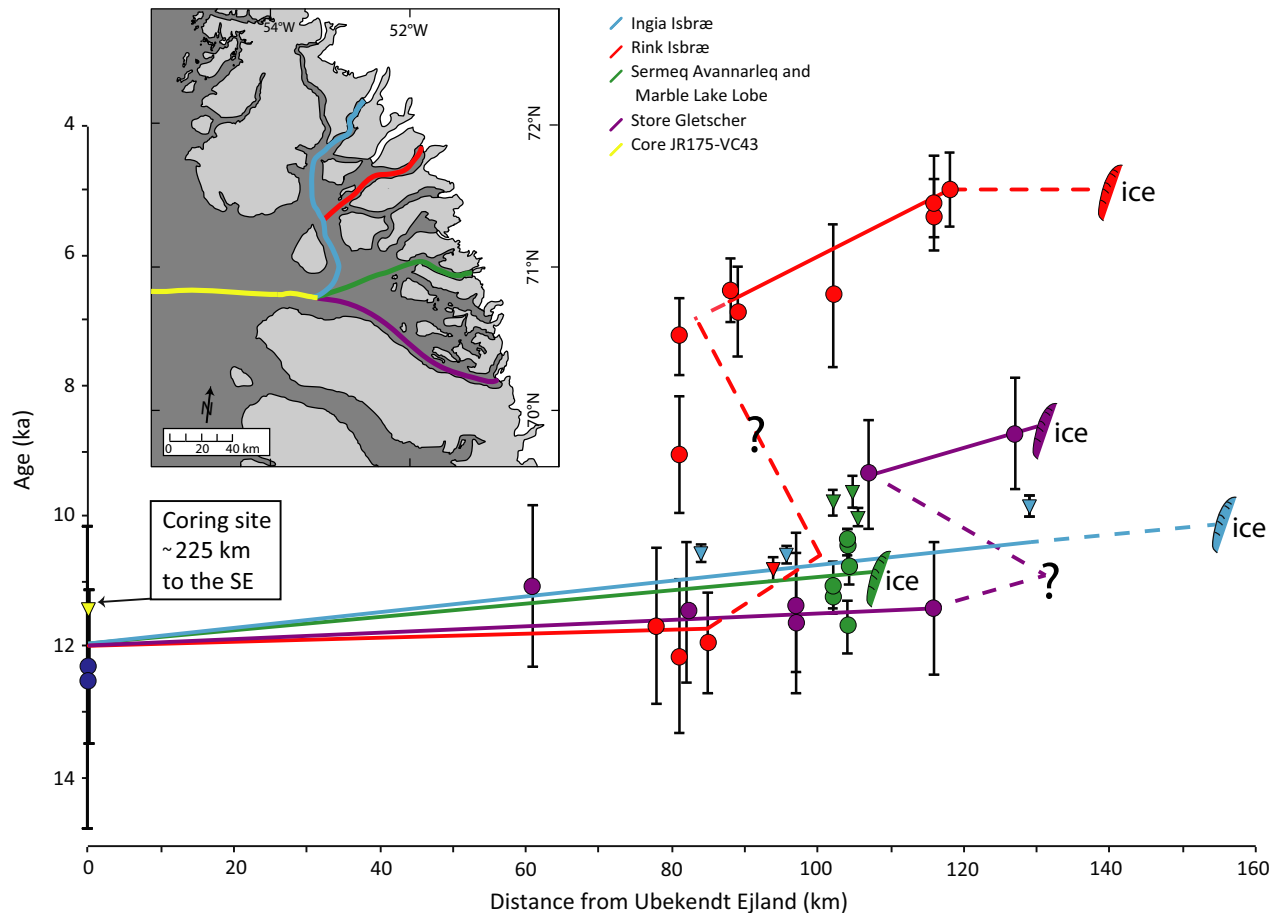


Fig. 10. Age models of deglaciation from the shelf break through Uummannaq's sub-fjords. Colour-coding is explained in the upper centre of the figure. Dots are cosmogenic nuclide exposure ages and triangles are ^{14}C deglaciation ages; black vertical bars on both indicate sample error. Half ovals represent the present-day ice margin. Lines model deglaciation excluding ages on Ubekendt Ejland. Lines depict ice-margin history of the Uummannaq Ice Stream System (shown in the upper left corner of this figure) and includes age listed on Fig. 1. Solid lines indicate constrained retreat rates and dashed lines inferred retreat rates. Question marks indicate inferred retreat rates. [Colour figure can be viewed at www.boreas.dk]

may relate to the onset of optimum oceanic conditions observed elsewhere in West Greenland *c.* 6–5 ka, which may have caused submarine melting of the ice front and destabilization of the terminus (Perner *et al.* 2012; Briner *et al.* 2014, 2016).

In summary, the existing chronology from the Uummannaq Fjord system indicates collapse of the Uummannaq Ice Stream system at *c.* 11.0 ka (Fig. 10). In some locations, ice retreated to very near to or within its current position (central Uummannaq, Store Gletscher, Inngia Isbræ), whereas ice stalled in outer Kangilleq until the middle Holocene. Considering the minimum age of deglaciation from the middle shelf at *c.* 11.5 ± 0.2 cal. ka BP (Sheldon *et al.* 2016), ~ 330 km from Sermeq Avannarleq and the Marble Lake Lobe margins, we estimate a net retreat rate between 300 and 1100 m a^{-1} (Fig. 10). Considering the ice stream may have drained $\sim 6\%$ of the GrIS during the LGM (Roberts *et al.* 2013), the GrIS would have experienced a substantial amount of ice loss in this brief period.

Timing of final deglaciation in central West Greenland

The deglaciation of the GrIS to or within its historical limit varied throughout central West Greenland. Here, we compare the deglaciation history of the Uummannaq Fjord system to other marine embayments in central West Greenland where detailed deglaciation chronologies are available. To the south of Uummannaq is Disko Bugt, with arguably one of the best constrained GrIS histories in all of Greenland, and to the north of Uummannaq lies Upernavik Isfjord where recent studies have provided a deglaciation chronology (Fig. 1).

Similar to in Uummannaq, the GrIS terminated on the continental shelf far west of Disko Bugt during the LGM (Ó Cofaigh *et al.* 2013). The deglaciation of the shelf is reconstructed using marine cores, indicating that a cycle of advance and retreat occurred in the Disko Trough during the Younger Dryas (Jennings *et al.* 2014; Rinterknecht *et al.* 2014; Hogan *et al.* 2016). Following retreat of ice from the shelf off Disko Bugt, there may

have been a halt in the deglaciation with an ice margin in western Disko Bugt. Disko Bugt seems to have deglaciated rapidly, perhaps related to an ice collapse due to its somewhat eastward-widening geometry and lack of islands that could function as anchor points (Kelley *et al.* 2013). ^{10}Be ages constrain the onset of ice-margin retreat from outer (western) Disko Bugt at 10.8 ± 0.5 ka, and onto the landscape east of Disko Bugt at 10.1 ± 0.3 ka (Kelley *et al.* 2013; Young *et al.* 2013a). This chronology yields a net retreat rate of $50\text{--}450 \text{ a}^{-1}$ for central Disko Bugt. The onset of deglaciation in outer Disko Bugt at 10.8 ± 0.5 ka is within error of our age of final deglaciation in central Uummannaq at 10.8 ± 0.2 ka, and thus Disko Bugt seems to have deglaciated *c.* 1 ka later than central Uummannaq Fjord (Kelley *et al.* 2013; Ó Cofaigh *et al.* 2013). However, there may have been comparable deglaciation rates.

Between Disko Bugt and the GrIS lie the Fjord Stade moraines, deposited at *c.* 9.2 and *c.* 8.2 ka, which delineate an important phase of the western GrIS's history (Young *et al.* 2013a). The moraines span from $\sim 64^\circ$ to 70°N , and have not been found in the Uummannaq Fjord system (Weidick 1968; Young & Briner 2015). After the collapse of ice in Disko Bugt, and following deposition of the Fjord Stade moraines, ice-margin retreat east of Disko Bugt resumed at rates of $\sim 100 \text{ m a}^{-1}$; the GrIS reached its present-day ice limit between *c.* 7.6 and 7.3 ka (Briner *et al.* 2010; Corbett *et al.* 2011). To the north of Jakobshavn Isfjord on the southern Nuussuaq peninsula, the Drygalski moraines, which lie directly adjacent to the present GrIS margin, date from 8.6 ± 0.4 to 7.6 ± 0.1 ka (Cronauer *et al.* 2016). The Fjord Stade and Drygalski moraines were deposited around the same time as the decrease in biological activity recorded in unit E2b in Erratic Lake that was deposited between *c.* 9.4 and 8.4 cal. ka BP. This timing is also consistent with the apparent halt of Store Gletscher (Roberts *et al.* 2013). The absence of mapped Fjord Stade moraines or equivalents in the Uummannaq Fjord system is consistent with the pre-Fjord-Stade timing of deglaciation we find in central Uummannaq. The Karrat-Nuugaatsiaq moraines mapped on Karrat Ø may be Fjord-Stade moraine equivalents, but existing chronology (*c.* 6 ka) suggests they are younger (Lane *et al.* 2014).

The next major marine glacier system north of Uummannaq is found at Upernavik Isfjord. Upernavik Isfjord deglaciated quickly around 11.3 ± 0.5 ka based on ^{10}Be ages of erratic boulders south of the fjord (Corbett *et al.* 2013). Near the present ice margin, ^{10}Be ages indicate that Upernavik Isfjord experienced final deglaciation at 9.9 ± 0.1 ka (Briner *et al.* 2013). This timing of deglaciation of Upernavik Isfjord *c.* 11–10 ka is consistent with the location being north of the range of the Fjord Stade moraines (i.e. it pre-dates the age of the Fjord Stade moraines) and is similar in age to the final deglaciation of central Uummannaq at 10.8 ± 0.2 ka.

Conclusions

We constrain ice retreat to the historical ice margin in the central Uummannaq Fjord system to *c.* 10.8 ka. Although final deglaciation across the Uummannaq Fjord system varied from *c.* 10.8 to *c.* 5.3 ka, all chronologies indicate a collapse from the continental shelf and through the middle Uummannaq fjords at *c.* 11 ka. We estimate a net retreat rate between 300 and 1100 m a^{-1} for the central sector of the Uummannaq Ice Stream system, which overlaps with the upper limit of the net retreat rate in central Disko Bugt. Although increasing atmosphere and oceanic temperatures would have prompted overall retreat, geometry effects related to trough width and depth no doubt led to rapid ice-margin recession, which our dating methods may be too uncertain to fully capture. The style of retreat of these large ice-stream systems in western Greenland may be analogous to future retreat for parts of the present-day Greenland and Antarctic ice sheets.

Acknowledgements. – We thank CPS polar field services for logistical support and the National Science Foundation grant ARC-1204005 and the National Science Foundation Graduate Research Fellowship Program (Fellow ID: 2013168643) for funding this work. Susan Zimmerman at the Center for Accelerator Mass Spectrometry (LLNL) was instrumental in producing precise ^{10}Be measurements; PRIME Lab personnel also assisted in providing a smaller portion of the ^{10}Be data set. We acknowledge National Science Foundation support for PRIME Lab from grant EAR-1153689. We thank Nicolaj Larsen and an anonymous reviewer for their helpful reviews.

References

- Alley, R. B., Andrews, J. T., Brigham-Grette, J., Clarke, G., Cuffey, K., Fitzpatrick, J., Funder, S., Marshall, S., Miller, G. & Mitrovica, J. 2010: History of the Greenland Ice Sheet: paleoclimatic insights. *Quaternary Science Reviews* 29, 1728–1756.
- Balco, G., Stone, J. O., Lifton, N. A. & Dunai, T. J. 2008: A complete and easily accessible means of calculating surface exposure ages or erosion rates from ^{10}Be and ^{26}Al measurements. *Quaternary Geochronology* 3, 174–195.
- Bennike, O. 2000: Palaeoecological studies of Holocene lake sediments from west Greenland. *Palaeogeography, Palaeoclimatology, Palaeoecology* 155, 285–304.
- Bennike, O. 2008: An early Holocene Greenland whale from Melville Bugt, Greenland. *Quaternary Research* 69, 72–76.
- Bennike, O. & Björck, S. 2002: Chronology of the last recession of the Greenland Ice Sheet. *Journal of Quaternary Science* 17, 211–219.
- Blaauw, M. 2010: Methods and code for 'classical' age-modelling of radiocarbon sequences. *Quaternary Geochronology* 5, 512–518.
- Boldt, B. R., Kaufman, D. S., McKay, N. P. & Briner, J. P. 2015: Holocene summer temperature reconstruction from sedimentary chlorophyll content, with treatment of age uncertainties, Kurupa Lake, Arctic Alaska. *The Holocene* 25, 641–650.
- Briner, J. P., Håkansson, L. & Bennike, O. 2013: The deglaciation and neoglaciation of Upernavik Isstrøm, Greenland. *Quaternary Research* 80, 459–467.
- Briner, J. P., Kaufman, D. S., Bennike, O. & Kosnik, M. A. 2014: Amino acid ratios in reworked marine bivalve shells constrain Greenland Ice Sheet history during the Holocene. *Geology* 42, 75–78.
- Briner, J. P., McKay, N. P., Axford, Y., Bennike, O., Bradley, R. S., de Vernal, A., Fisher, D., Francus, P., Fréchette, B., Gajewski, K., Jennings, A., Kaufman, D. S., Miller, G. H., Rouston, C. & Wegener, B. 2016: Holocene climate change in Arctic Canada and Greenland. *Quaternary Science Reviews* 147, 340–364.

- Briner, J., Stewart, H., Young, N., Philipps, W. & Losee, S. 2010: Using proglacial-threshold lakes to constrain fluctuations of the Jakobshavn Isbræ ice margin, western Greenland, during the Holocene. *Quaternary Science Reviews* 29, 3861–3874.
- Briner, J. P., Young, N. E., Goehring, B. M. & Schaefer, J. M. 2012: Constraining Holocene ^{10}Be production rates in Greenland. *Journal of Quaternary Science* 27, 2–6.
- Carlson, A. E., Winsor, K., Ullman, D. J., Brook, E. J., Rood, D. H., Axford, Y., LeGrande, A. N., Anslow, F. S. & Sinclair, G. 2014: Earliest Holocene south Greenland ice sheet retreat within its late Holocene extent. *Geophysical Research Letters* 41, 5514–5521.
- Clark, P. U., Dyke, A. S., Shakun, J. D., Carlson, A. E., Clark, J., Wohlfarth, B., Mitrovica, J. X., Hostetler, S. W. & McCabe, A. M. 2009: The last glacial maximum. *Science* 325, 710–714.
- Corbett, L. B., Bierman, P. R., Graly, J. A., Neumann, T. A. & Rood, D. H. 2013: Constraining landscape history and glacial erosivity using paired cosmogenic nuclides in Upernavik, northwest Greenland. *Geological Society of America Bulletin* 125, 1539–1553.
- Corbett, L. B., Young, N. E., Bierman, P. R., Briner, J. P., Neumann, T. A., Rood, D. H. & Graly, J. A. 2011: Paired bedrock and boulder ^{10}Be concentrations resulting from early Holocene ice retreat near Jakobshavn Isfjord, western Greenland. *Quaternary Science Reviews* 30, 1739–1749.
- Cronauer, S. L., Briner, J. P., Kelley, S. E., Zimmerman, S. R. & Morlighem, M. 2016: ^{10}Be dating reveals early-middle Holocene age of the Drygalski Moraines in central West Greenland. *Quaternary Science Reviews* 147, 59–68.
- Fredskild, B. 1985: The Holocene vegetational development of Tugtulligssuaq and Qeqertat, Northwest Greenland. *Meddelelser om Grønland, Geoscience* 14, 1–20.
- Funder, S., Kjeldsen, K. K., Kjær, K. H. & Ó Cofaigh, C. 2011: The Greenland Ice Sheet during the past 300,000 years: a review. *Developments in Quaternary Science* 15, 699–713.
- Håkansson, L., Briner, J. P., Andresen, C. S., Thomas, E. K. & Bennike, O. 2014: Slow retreat of a land based sector of the West Greenland Ice Sheet during the Holocene Thermal Maximum: evidence from threshold lakes at Paakitsoq. *Quaternary Science Reviews* 98, 74–83.
- Hogan, K. A., Ó Cofaigh, C., Jennings, A. E., Dowdeswell, J. A. & Hiemstra, J. F. 2016: Deglaciation of a major palaeo-ice stream in Disko Trough, West Greenland. *Quaternary Science Reviews* 147, 5–26.
- Jennings, A. E., Walton, M. E., Ó Cofaigh, C., Kilfeather, A., Andrews, J. T., Ortiz, J. D., De Vernal, A. & Dowdeswell, J. A. 2014: Palaeoenvironments during Younger Dryas-Early Holocene retreat of the Greenland Ice Sheet from outer Disko Trough, central west Greenland. *Journal of Quaternary Science* 29, 27–40.
- Kelley, S. E., Briner, J. P. & Young, N. E. 2013: Rapid ice retreat in Disko Bugt supported by ^{10}Be dating of the last recession of the western Greenland Ice Sheet. *Quaternary Science Reviews* 82, 13–22.
- Lal, D. 1991: Cosmic ray labeling of erosion surfaces: in situ nuclide production rates and erosion models. *Earth and Planetary Science Letters* 104, 424–439.
- Lane, T. P., Roberts, D. H., Rea, B. R., Ó Cofaigh, C., Vieli, A. & Rodés, A. 2014: Controls upon the Last Glacial maximum deglaciation of the northern Uummannaq ice stream system, West Greenland. *Quaternary Science Reviews* 92, 324–344.
- Larsen, N. K., Funder, S., Kjær, K. H. & Kjeldsen, K. K. 2014: Rapid early Holocene ice retreat in West Greenland. *Quaternary Science Reviews* 92, 310–323.
- Larsen, N. K., Kjær, K. H., Lecavalier, B., Bjørk, A. A., Colding, S., Huybrechts, P., Jakobsen, K. E., Kjeldsen, K. K., Knudsen, K. L., Odgaard, B. V. & Olsen, J. 2015: The response of the southern Greenland ice sheet to the Holocene thermal maximum. *Geology* 43, 291–294.
- Larsen, N. K., Kjær, K. H., Olsen, J., Funder, S., Kjeldsen, K. K. & Nørgaard-Pedersen, N. 2011: Restricted impact of Holocene climate variations on the southern Greenland Ice Sheet. *Quaternary Science Reviews* 30, 3171–3180.
- Levy, L., Kelly, M. A., Howley, J. A. & Virginia, R. A. 2012: Age of the Orkendalen moraines, Kangerlussuaq, Greenland: constraints on the extent of the southwestern margin of the Greenland Ice Sheet during the Holocene. *Quaternary Science Reviews* 52, 1–5.
- Lifton, N., Beel, C., Hättetrstrand, C., Kassab, C., Rogozhina, I., Heermance, R., Oskin, M., Burbank, D., Blomdin, R. & Gribenski, N. 2014: Constraints on the late Quaternary glacial history of the Inylchek and Sary-Dzaz valleys from in situ cosmogenic ^{10}Be and ^{26}Al , eastern Kyrgyz Tian Shan. *Quaternary Science Reviews* 101, 77–90.
- Michelutti, N., Blais, J. M., Cumming, B. F., Paterson, A. M., Rühland, K., Wolfe, A. P. & Smol, J. P. 2010: Do spectrally inferred determinations of chlorophyll a reflect trends in lake trophic status? *Journal of Paleolimnology* 43, 205–217.
- Morlighem, M., Rignot, E., Mouginot, J., Seroussi, H. & Larour, E. 2014: Deeply incised submarine glacial valleys beneath the Greenland ice sheet. *Nature Geoscience* 7, 418–422.
- Nishiizumi, K., Imamura, M., Caffee, M., Southon, J., Finkel, R. & McAninch, J. 2007: Absolute calibration of ^{10}Be AMS standards. *Nuclear Instruments and Methods in Physical Research Section B: Beam Interactions with Materials and Atoms* 258, 403–413.
- Ó Cofaigh, C., Dowdeswell, J., Jennings, A., Hogan, K., Kilfeather, A., Hiemstra, J., Noormets, R., Evans, J., McCarthy, D. & Andrews, J. 2013: An extensive and dynamic ice sheet on the West Greenland shelf during the last glacial cycle. *Geology* 41, 219–222.
- Overpeck, J. T., Otto-Bliesner, B. L., Miller, G. H., Muhs, D. R., Alley, R. B. & Kiehl, J. T. 2006: Paleoclimatic evidence for future ice-sheet instability and rapid sea-level rise. *Science* 311, 1747–1750.
- Perner, K., Moros, M., Jennings, A., Lloyd, J. M. & Knudsen, K. L. 2012: Holocene palaeoceanographic evolution off West Greenland. *The Holocene* 23, 374–387.
- Reeh, N. 1985: Was the Greenland ice sheet thinner in the late Wisconsinan than now? *Nature* 317, 797–799.
- Rein, B. & Sirocko, F. 2002: In-situ reflectance spectroscopy—analysing techniques for high-resolution pigment logging in sediment cores. *International Journal of Earth Sciences* 91, 950–954.
- Rignot, E., Fenty, I., Xu, Y., Cai, C. & Kemp, C. 2015: Undercutting of marine-terminating glaciers in West Greenland. *Geophysical Research Letters* 42, 5909–5917.
- Rignot, E., Fenty, I., Xu, Y., Cai, C., Velicogna, I., Ó Cofaigh, C., Dowdeswell, J., Weinrebe, W., Catania, G. & Duncan, D. 2016: Bathymetry data reveal glaciers vulnerable to ice-ocean interaction in Uummannaq and Vaigat glacial fjords, west Greenland. *Geophysical Research Letters* 43, 2667–2674.
- Rinterknecht, V., Jomelli, V., Brunstein, D., Favier, V., Masson-Delmotte, V., Bourlès, D., Leanni, L. & Schläpky, R. 2014: Unstable ice stream in Greenland during the Younger Dryas cold event. *Geology* 42, 759–762.
- Roberts, D. H., Rea, B. R., Lane, T. P., Schnabel, C. & Rodés, A. 2013: New constraints on Greenland ice sheet dynamics during the last glacial cycle: evidence from the Uummannaq ice stream system. *Journal of Geophysical Research: Earth Surface* 118, 519–541.
- Rood, D. H., Hall, S., Guilderson, T. P., Finkel, R. C. & Brown, T. A. 2010: Challenges and opportunities in high-precision Be-10 measurements at CAMS. *Nuclear Instruments and Methods in Physics Research Section B: Beam Interactions with Materials and Atoms* 268, 730–732.
- Sheldon, C., Jennings, A., Andrews, J., Ó Cofaigh, C., Hogan, K., Seidenkrantz, M.-S. & Dowdeswell, J. 2016: Ice stream retreat following the LGM and onset of the West Greenland Current in Uummannaq Trough, West Greenland. *Quaternary Science Reviews* 147, 27–46.
- Sinclair, G., Carlson, A. E., Mix, A. C., Lecavalier, B. S., Milne, G., Mathias, A., Buizert, C. & DeConto, R. 2016: Diachronous retreat of the Greenland ice sheet during the last deglaciation. *Quaternary Science Reviews* 145, 243–258.
- Stone, J. O. 2000: Air pressure and cosmogenic isotope production. *Journal of Geophysical Research: Solid Earth* 105, 23753–23759.
- Velicogna, I. & Wahr, J. 2006: Acceleration of Greenland ice mass loss in spring 2004. *Nature* 443, 329–331.
- Weidick, A. 1968: Observations on some Holocene glacier fluctuations in West Greenland. *Meddelelser om Grønland* 165, 202 pp.
- Weidick, A. 1978: ^{14}C dating of survey material carried out in 1977. *Rapport Grønlands Geologiske Undersøgelse* 90, 119–124.
- Weidick, A., Bennike, O., Citterio, M. & Nørgaard-Pedersen, N. 2012: Neoglacial and historical glacier changes around Kangersuneq fjord

- in southern West Greenland. *Geological Survey of Denmark and Greenland Bulletin* 27, 68 pp.
- Wolfe, A. P., Vinebrooke, R. D., Michelutti, N., Rivard, B. & Das, B. 2006: Experimental calibration of lake-sediment spectral reflectance to chlorophyll a concentrations: methodology and paleolimnological validation. *Journal of Paleolimnology* 36, 91–100.
- Young, N. E. & Briner, J. P. 2015: Holocene evolution of the western Greenland Ice Sheet: assessing geophysical ice-sheet models with geological reconstructions of ice-margin change. *Quaternary Science Reviews* 114, 1–17.
- Young, N. E., Briner, J. P., Rood, D. H., Finkel, R. C., Corbett, L. B. & Bierman, P. R. 2013a: Age of the Fjord Stade moraines in the Disko Bugt region, western Greenland, and the 9.3 and 8.2 ka cooling events. *Quaternary Science Reviews* 60, 76–90.
- Young, N. E., Schaefer, J. M., Briner, J. P. & Goehring, B. M. 2013b: A ^{10}Be production-rate calibration for the Arctic. *Journal of Quaternary Science* 28, 515–526.